Production conditions and fine structure parameters of metallic glasses based on light rare-earth elements

A.B. Lysenko, T.V. Kalinina, A.-M.V. Tomina, Y.V. Vishnevskaya, O.I. Popil

Department of Condensed Matter Physics, Dniprovsk State Technical University, Kamyanske, Ukraine

E-mail: ablysenko@ukr.net

Abstract. Thermal regimes of formation and parameters of the fine structure of amorphous alloys based on light rare-earth elements (E-La, Ce, Pr) with normal metals (M-Al, Cu, Ag) obtained by rapid cooling of melt layers on the inner surface of a rotating cylindrical heat receiver are studied. It has been shown that the alloys under study belong to materials with an average level of glass-forming ability (GFA), whichsolidify without crystallization in cross sections from 35 to 65 μm during quenching from a liquid state. Based on the correlation between the sizes of coherent scattering regions and the shortest interatomic distances found by X-ray diffraction for E-M amorphous alloys with the corresponding characteristics of metallic glasses of other classes, a conclusion was made about a close analogy of the atomic structure of noncrystalline phases fixed by quenching metallic melts.

1. Introduction

As is known, during quenching from a liquid state (QLS), the processes of formation of the structure of alloys occur under nonequilibrium conditions and are accompanied by the fixation of metastable phases of various types. These include, in particular, structures without long-range order in the arrangement of atoms, which give diffuse patterns of X-ray and electron scattering [1-3]. Alloys with a similar structure are called amorphous or metallic glasses (MGs). They have unique sets of properties, as a result of which they are widely used in modern technology. Subject to the foregoing, expanding the list of amorphous alloys, determining the conditions for non-crystalline solidification, and studying the fine structure and properties of MGs are topical problems of metal physics and materials science. Among the listed problems, a special place is occupied by the development of methods for controlling the rate of quenching from the liquid state υ [4-6], that determines the degree of metastability of the structure and is a quantitative characteristic of the glass-forming ability of materials.

In this work, the value υ was calculated from the thickness l of rapidly quenched samples using the ratios $\lg\upsilon(\lg l)$ obtained by the authors [5] by matching the results of the numerical solution of the heat conduction equations with a wide array of corresponding experimental estimates. The calculation algorithm [5] was used to determine the critical cooling rates υ_c, which cause non-crystalline solidification of alloys of light rare earth elements (E-La, Ce, Pr) with normal metals (M-Al, Cu, Ag),

as well as to analyze the relative tendency to amorphization both between the alloys of the group under study and in comparison with well-known vitrifying alloys of other classes.

2. Materials and methods of the research

We have chosen alloys for studying the conditions for the formation and details of the structure of metallic glasses on basis of the following considerations. Firstly, for light lanthanides, which form the compositional basis of $E_{100-x}M_x$ alloys (where x is the atomic concentration of the alloying element), the temperature dependences of thermophysical properties (specific heat capacity, density, thermal conductivity) in the solid and liquid states are known [7-9], that increases the correctness of the results of the computational analysis of the speed of the process of the QLS.

Secondly, the components of the selected alloys have significantly different atomic sizes. For example, for alloys based on lanthanum, the relative differences in Goldschmidt atomic radii vary within $(r_E\text{-}r_M)/r_E$=0,230-0,316. These values are consistent with the size factor (0,2-0,3) of many vitrifying alloys [10], and make it possible to expect the formation of amorphous structures in rapidly quenched E–M alloys.

Thirdly, a common feature of the state diagrams of the E-M systems is the almost complete absence of mutual solubility of the components in the solid state and the presence of several intermediate phases of constant composition (chemical compounds), which participate in eutectic transformations at the final stages of alloy solidification. Transformations involving the main component and the chemical compound closest to it have the lowest temperature. These transformations are also characterized by the maximum length of the concentration interval ΔC_E separating the eutectic phases. In particular, in alloys of lanthanum with aluminum, copper and silver, the coordinates of low-temperature eutectics (T_E, C_E) and the value of ΔC_E are, respectively: 820 K, 23%Al; 748 K, 29%Cu; 808 K, 23,5%Ag and 25%Al; 50%Cu; 50%Ag. As it is known, the presence of "deep" eutectics in state diagrams is a sign of the tendency of alloys to amorphization [11]. The probability of non-crystalline solidification increases with an increase of ΔC_E value, and also in cases when incongruent compounds are involved in the eutectic transformation [12].

The combination of the factors considered above leads to the conclusion that the alloys of the E–M systems belonging to the regions of low-temperature eutectics can be used to study the conditions of non-crystalline solidification and X-ray analysis of structural details of metallic glasses.

The alloys under study were smelted from rare-earth metals with a total impurity content of no more than 1%: AB000 aluminum, electrolytic copper, and spectrally pure silver in a vacuum electric furnace at residual pressure of $6{,}65\cdot10^{-3}$ Pa. Quenching from the liquid state was carried out by injecting a small portion (~100 mg) of superheated melt onto the inner surface of a rapidly rotating (up to 6000 rpm) bronze cylinder.As a result of collision with the cylinder and under the action of centrifugal forces, the melt spread over the hardening surface and solidified in the form of foils with a thickness of 20-80 μm. The use of chemically pure argon as an injection gas and the rapidity of the melt solidification process made it possible to obtain foils with shiny surfaces without noticeable traces of interaction with the air.

The structure of rapidly quenched foils was studied by X-ray diffraction. X-ray scattering patterns were recorded in the range of reflection angles 2θ from 15 to 100° on a DRON-3 diffractometer in monochromatized $Mo_{K\alpha}$ radiation. From the quantitative characteristics of the first halo on the diffraction patterns of rapidly quenched amorphous $E_{100-x}M_x$ alloys, we determined the effective sizes of coherent scattering regions L and the shortest interatomic distances d_0, which are usually considered as parameters of the fine structure of metallic glasses.

3. Results of the research and their analysis

In order to determine the critical regimes of QLS that cause amorphization of E-M alloys, we analyzed the dependences of the cooling rate on the thickness of rapidly quenched foils. The values of υ were calculated according to the method of the work [5], which is based on the following provisions:

1. The most significant factors that determine the value of υ are the thickness of the melt layer l and heat transfer coefficient α at the melt-substrate interface. The relationship between the parameters υ, l, α is described by the ratio:

$$\lg \upsilon = 2{,}7 + \lg(\alpha / l) \qquad (1)$$

2. There is no single value of α suitable for calculating the cooling rate of products of rapid quenching of any thickness, obtained by different methods of QLS.

3. Parameters l and α are not independent technological variables. Under real conditions of QLS, the decrease in the thickness of the melt layers is accompanied by an improvement in the quality of its thermal contact with the quenching block, that is, by an increase in the heat transfer coefficient α.

4. In various intervals of l values, which can relate to three groups of rapid quenching methods, namely, the most dynamic "shot" method (l<20 μm), various modifications of themethod of quenching the melt on moving substrates (20≤l≤100 μm) and methods of casting into a metal mold (l>100 μm), the dependences $\alpha(l)$ have a specific character, they demonstrate a general growth trend of α with decreasing in l:

$$\lg \alpha = \begin{cases} 5{,}4 - 0{,}7 \lg l, \text{for} \quad l > 100\,\mu\text{m} \\ 7{,}9 - 1{,}9 \lg l, \ \text{for} \, 20 \le l \le 100\,\mu\text{m} \\ 5{,}8 - 0{,}3 \lg l, \text{for} \quad l < 20\,\mu\text{m} \end{cases} \qquad (2)$$

By the combination of equations (1) and (2) in the cited paper [5], one-parameter ratios are obtained; they allow one to calculate the melt cooling rate over the thickness of rapidly quenched samples, which can be easily determined experimentally:

$$\lg \upsilon = \begin{cases} 8{,}1 - 1{,}7 \lg l, \quad \text{for} \quad l > 100\,\mu\text{m} \\ 10{,}5 - 2{,}9 \lg l, \text{for} \, 20 \le l \le 100\,\mu\text{m} \\ 8{,}4 - 1{,}3 \lg l, \quad \text{for} \quad l < 20\,\mu\text{m} \end{cases} \qquad (3)$$

Table 1 shows the values of the cooling rate calculated by ratios (3), as well as the experimental estimates of the value of υ obtained by various authors collected in a single array in [13]. Comparison of the calculated and experimental data indicates their good agreement over the entire range of thicknesses of rapidly quenched products, which are obtained by known methods of quenching from a liquid state.

The results of calculations and experimental measurements of the value of υ are shown in graphical format in Figure 1 for QLS-foils, tapes or flakes with a thickness from 20 to 100 μm, which are obtained by methods of rapid cooling of melt layers on movable quenching devices including the method used in this work. As can be seen, the experimental points are grouped around the calculated dependence with an acceptable spread of lgυ±0,4 values for the difficult-to-determine parameter υ, which indicates the reliability of the υ values calculated by the ratios (3) for melt layers of different thicknesses.

Concluding the analysis of Figure 1 we note that in accordance with the slope of the calculated line, the parameters υ and l are related to each other by a power dependence of $\upsilon \sim l^{-2,9}$ form, which practically coincides with the function $\upsilon \sim l^{-3,1}$ obtained by the authors of the work [4] according to the results of experimental studies of the cooling regime in the method of spinning the melt. This fact gives additional grounds for the conclusion about the correctness of the algorithm used to determine the speed of the process of QLS.

Table 1. Calculated and experimental cooling rates for melt layers of different thicknesses.

Calculation according to (3)		Experiment [13]	
l, μm	υ,K/s	l, μm	υ,K/s
1,0	$2{,}5\cdot10^{8}$	~1,0	$(1\text{-}5)\cdot10^{8}$
20	$5{,}4\cdot10^{6}$	18; ~20	$8{,}5\cdot10^{6}$; $1{,}5\cdot10^{6}$
25	$2{,}8\cdot10^{6}$	24±3; 25; 27	$3{,}3\cdot10^{6}$; $4{,}0\cdot10^{6}$; 10^{6}
30	$1{,}7\cdot10^{6}$	30; 30±3; 31	$2{,}2\cdot10^{5}$; $1{,}2\cdot10^{6}$; $8{,}0\cdot10^{5}$
35	$1{,}1\cdot10^{6}$	35±7,5	$4{,}5\cdot10^{5}$
40	$7{,}1\cdot10^{5}$	40±7,5	$3{,}1\cdot10^{5}$
45	$5{,}1\cdot10^{5}$	44; 44; 45±7,5	$1{,}2\cdot10^{6}$; $7{,}8\cdot10^{5}$; $1{,}5\cdot10^{5}$
60	$2{,}2\cdot10^{5}$	61	$1{,}7\cdot10^{5}$
65	$1{,}7\cdot10^{5}$	65; 65±5	$9{,}7\cdot10^{4}$; $1{,}8\cdot10^{5}$
70	$1{,}4\cdot10^{5}$	67,5±7,5; 70	$8{,}1\cdot10^{4}$; $6{,}9\cdot10^{5}$;
95	$5{,}8\cdot10^{4}$	95±10	$4{,}0\cdot10^{4}$
100	$5{,}0\cdot10^{4}$	100-150	$4{,}0\cdot10^{4}$
150	$2{,}5\cdot10^{4}$		
250	$1{,}1\cdot10^{4}$	250	$8{,}0\cdot10^{3}$
1000	10^{3}	1040	$9{,}7\cdot10^{2}$
2100	$2{,}8\cdot10^{2}$	2100	$(1\text{-}3)\cdot10^{2}$

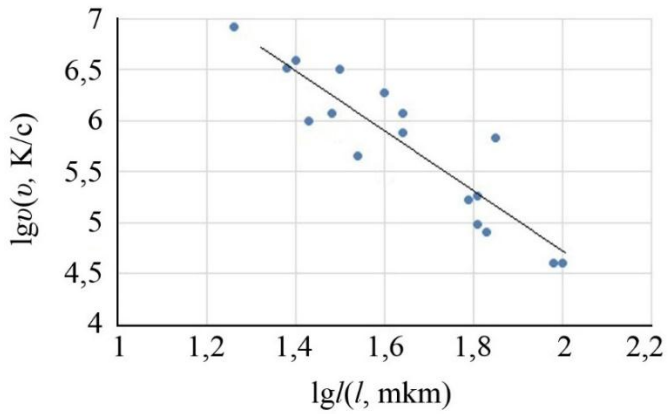

Figure 1. The dependence of the rate of quenching from the liquid state on the thickness $20 \le l \le 100$ μm of melt layers: solid line – calculation by ratio (3); dots are experimental estimates.

In the experimental block of studies, the critical values of l_c thickness of QLS products were determined, at which the crystallization processes are suppressed and structures typical of metallic glasses are fixed in $E_{100-x}M_x$ alloys. For this purpose, rapidly-quenched foils were made, the thickness of which for each alloy studied varied from ~ 25 μm ($\upsilon \simeq 3\cdot10^{6}$ K/s) to ~ 80 μm ($\upsilon \simeq 10^{5}$ K/s). The structure of the foils was monitored radiographically to determine the maximum (critical) thickness of the samples, that give purely diffuse patterns of X-ray scattering.

On Figure 2–4 diffraction patterns of rapidly quenched foils of $E_{100-x}Al_x$, $E_{100-x}Cu_x$ and $E_{100-x}Ag_x$ alloys are shown, respectively. It can be seen that, with the exception of $Pr_{73}Ag_{27}$ alloy (Figure 4, c), the diffraction patterns contain only 3 diffuse maxima located in the $\sin\theta/\lambda$ range from 1 to 5 nm^{-1}, where θ is the reflection angle; λ is the X-ray wavelength. In general terms, the presented diffraction patterns are similar to the patterns of X-ray scattering by liquid metals and alloys [14]; that

allows us to conclude that the studied samples lack long-range order in the arrangement of atoms, which is characteristic of crystalline materials.

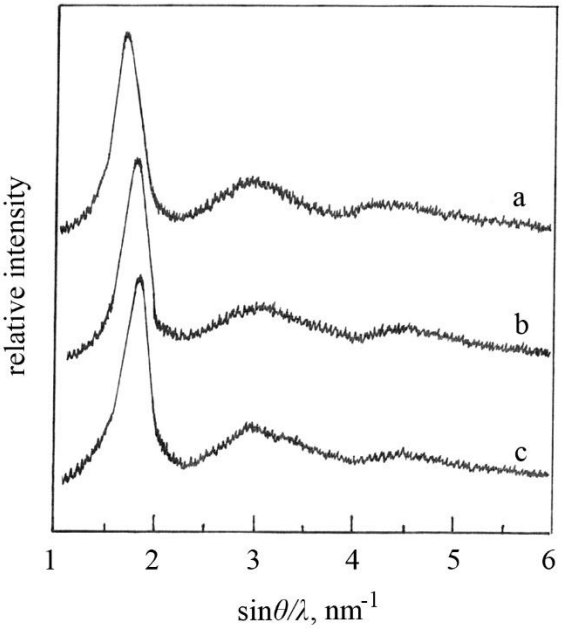

Figure 2. Typical diffraction patterns of rapidly quenched E-Al alloys:
a – $La_{80}Al_{20}$, $\upsilon \simeq 6 \cdot 10^5$K/s;b – $Ce_{70}Al_{30}$, $\upsilon \simeq 6 \cdot 10^5$K/s; c – $Pr_{65}Al_{35}$, $\upsilon \simeq 8 \cdot 10^5$K/s.

As noted above, such structures are called amorphous, and the corresponding rapidly quenched alloys are called metallic glasses (MGs). Using this terminology, it is necessary to understand that in reality metallic glasses have a composite structure. According to the results of numerous studies, including [3], they contain a negligibly small volume fraction of the nanocrystalline component (so-called "quenching germs"), which does not exceed the sensitivity level of X-ray phase analysis ($\sim 10^{-2}$); as a result it is not detected by this method.

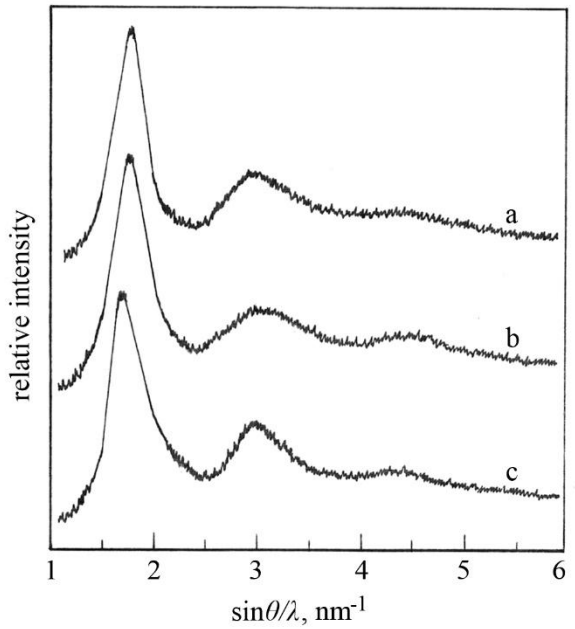

Figure 3. X-ray diffraction patterns of E-Cu alloys quenched from the liquid state at a rate of $\upsilon \simeq 3 \cdot 10^5$ K/s: a – $La_{74}Cu_{26}$; b – $Ce_{72}Cu_{28}$; c – $Pr_{68}Cu_{32}$.

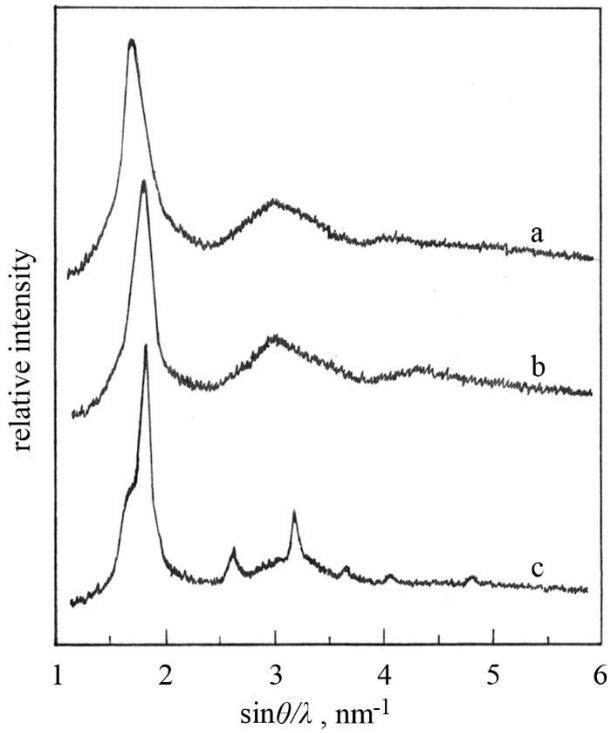

Figure 4. Diffractograms of rapidly quenched E-Ag alloys:
a – $La_{71}Ag_{29}$, $\upsilon \simeq 1{,}7 \cdot 10^6$K/s; b – $Ce_{79}Ag_{21}$, $\upsilon \simeq 1{,}1 \cdot 10^6$K/s; c – $Pr_{73}Ag_{27}$, $\upsilon \simeq 2 \cdot 10^6$K/s.

By processing of X-ray diffraction patterns obtained from $E_{100-x}M_x$ QLS-alloys, it was found that they have a number of common features with diffraction patterns of amorphous materials of other classes, made both by quenching the melts and by vacuum deposition, chemical or electrolytic deposition. The mentioned similarity can be noticed because of the fact that, firstly, regardless of the nature of the components and the method of fixing the non-crystalline state, the coordinates of the first two maxima are related with good accuracy by the ratio: $\sin\theta_2/\sin\theta 1 \simeq 1{,}7$. In particular, this ratio varies within 1,65-1,72 for rapidly quenched alloys (Table 2). Secondly, a "shoulder" is revealed on the descending branch of the second maximum for the majority of MGs studied by X-ray diffraction; that is a very common feature of the diffractograms of amorphous substances. In a number of alloys under study, this feature of the shape of X-ray scattering curves is most clearly observed in the diffraction patterns of rapidly quenched $Pr_{65}Al_{35}$ (Figure 2, c) and $Ce_{79}Ag_{21}$ (Figure 4, b) foils. Finally, thirdly, the diffraction patterns of metallic glasses of different classes are characterized by a fairly close degree of diffuseness, the quantitative indicator of which is the width β of the first halo measured at the middle of its height.

The sizes L of coherent scattering region (CSR) were calculated using the value of β according to Selyakov–Scherrer relation [15]. These regions have the meaning of one of the quantitative characteristics of the fine structure of metallic glasses:

$$L = \frac{\lambda}{\beta \cdot \cos\theta_1}. \qquad (4)$$

As can be seen from Table 2, the CSR sizes are (1,15-1,85) nm for rapidly quenched amorphous $E_{100-x}M_x$ alloys. The lower part of this interval includes the values L=(1,15-1,40) nm, that is inherent

for metallic glasses of E-Cu systems. Higher values of the parameter L=(1,59-1,85) nm were recorded for rapidly quenched amorphous E-Al and E-Ag alloys. In general, the range of values L, reflected in the Table 2, are applied to the E-M alloys under study; it is consistent with the corresponding estimates for amorphous alloys of other systems published in the literature; that indicates a close analogy of their atomic structure.

Table 2. Quantitative characteristics of X-Ray diffraction patterns and fine structure parameters of $E_{100-x}M_x$ metallic glasses.

Alloy	$\frac{\sin\theta_1}{\lambda}$, nm^{-1}			$\frac{\sin\theta_2}{\sin\theta_1}$	L, nm	d_0, nm	$d_0^{'}$, nm	$\frac{d_0 - d_0^{'}}{d_0}$	l_c, μm	υ_c, K/s
	i=1	i=2	i=3							
$La_{80}Al_{20}$	1,71	2,94	4,26	1,71	1,69	0,360	0,357	0,008	45	$5\cdot10^5$
$Ce_{70}Al_{30}$	1,79	3,02	4,32	1,69	1,70	0,344	0,340	0,012	45	$5\cdot10^5$
$Pr_{65}Al_{35}$	1,79	2,96	4,34	1,65	1,59	0,344	0,337	0,020	40	$7\cdot10^5$
$La_{74}Cu_{26}$	1,74	2,96	4,30	1,70	1,40	0,353	0,343	0,028	60	$2{,}2\cdot10^5$
$Ce_{72}Cu_{28}$	1,77	3,02	4,29	1,70	1,31	0,347	0,334	0,037	62	$2\cdot10^5$
$Pr_{68}Cu_{32}$	1,78	3,02	4,31	1,69	1,15	0,346	0,329	0,046	65	$1{,}8\cdot10^5$
$La_{71}Ag_{29}$	1,74	2,99	4,00	1,72	1,63	0,353	0,349	0,011	35	$1{,}1\cdot10^6$
$Ce_{79}Ag_{21}$	1,77	3,03	4,35	1,71	1,85	0,347	0,348	-0,003	37	$9\cdot10^5$

Another structural parameter of metallic glasses, the value of the shortest interatomic distance do d_0 was determined using the Ehrenfest formula [14]:

$$d_0 = \frac{0{,}615\cdot\lambda}{\sin\theta_1}. \qquad (5)$$

In Table 2 the results of calculations of the value of d_0 for amorphous E-M alloys are given along with the distances between the nearest atoms $d_0^{'}$, which were obtained by linear interpolation of the corresponding values of pure components:

$$d_0^{'} = (1-\frac{x}{100})d_0^{E} + \frac{x}{100}d_0^{M}, \qquad (6)$$

where d_0^{E} and d_0^{M} are, respectively, the smallest interatomic distances in the crystal lattices of the rare-earth and alloying elements.

As can be seen from a comparison of the values of d_0 and $d_0^{'}$, the formation of non-crystalline phases during quenching from the liquid state of alloys based on light lanthanides is not accompanied by a significant change in the distances between the nearest atoms in comparison with equilibrium close-packed structures. At the same time, a predominantly higher (by 0,8-4,5%) level of d_0 values found from the diffraction patterns of $E_{100-x}M_x$ metallic glasses can be interpreted as evidence of loosening of the atomic packing during non-crystalline solidification of melts.

In addition to information about the details of X-ray diffraction patterns and the values of the structural parameters (L, d_0) of metallic glasses, Table 2 presents the results of a comparative analysis of the conditions for amorphization of the studied E-M alloys. In quantitative terms, these conditions are characterized by the critical values of the thickness l_c and cooling rate υ_c of the melt layers, at which structures are fixed without X-ray signs of crystallinity.

According to the data in Table 2, E-Cu alloys demonstrate the greatest predisposition to amorphization, for them the critical parameters are: l_c=(60-65) μm, υ_c=$2\cdot10^5$K/s. The critical sections of the amorphizing foils for alloys of the E-Al system are reduced to the values l_c=(40-45) μm, which

correspond to the cooling rates $\upsilon_c \simeq (5\text{-}7)\ 10^5$ K/s. The lowest level of glass-forming ability is recorded in alloys of rare-earth elements with silver. For La-Ag and Ce-Ag alloys, the parameters l_c and υ_c are ~36 μm and ~10^6 K/s, and in the $Pr_{73}Ag_{27}$ eutectic alloy an amorphous structure is formed only in the so-called "whiskers", that is, filament-like samples with a thickness of less than 10 μm, the cooling rate of which exceeds the level of ~10^7 K/s. Diffraction patterns from such samples, obtained by the photomethod in the X-ray Debye camera, have a purely diffuse appearance indicating the absence of a crystalline phase in the structure of the alloy in an amount that is sufficient for X-ray identification.

In order to estimate the relative tendency of E-M alloys to amorphization, we used the following approach [16]: according to the level of glass-forming ability, metal materials belong to one of four groups: 1) materials (Al, Cu,…) materials (Al, Cu,…) that do not demonstrate the ability to non-crystalline solidification at all experimentally achievable cooling rates (up to ~10^{11} K/s); 2) materials (Ni, Ge,…) with minimal GFA amorphized in layers less than 1 μm thick under extreme conditions (~10^9-10^{10} K/s) of rapid quenching; 3) alloys with an average level of GFA, obtained in the form of amorphous ribbons, foils, flakes with a thickness of (25-70) μm by various QLS methods; 4) alloys with high GFA amorphizing in sections of more than 1 mm while casting into a metal mold ($Mg_{65}Cu_{25}Y_{10}$, $Zr_{41,2}Ti_{13,8}Cu_{12,5}Ni_{10}Be_{22,5}$,…).

The values of the critical thickness (35-65 μm) of amorphous foils of alloys of light lanthanides (La, Ce, Pr) with normal metals (Al, Cu, Ag) presented in Table 2 indicate that, in general, the alloys under study belong to materials of the third group with an average glass-forming ability. A typical example of materials of this group is $Fe_{80}B_{20}$ alloy, from which amorphous ribbons with a cross section of up to ~43 mm are made by melt spinning method.

To conclude the analysis of the glass-forming ability of E-M alloys, we present experimental data that are beyond the scope of this work and concern the possibility of non-crystalline solidification of E-Al alloys with an increased aluminum content regarding the composition of low-temperature eutectics. In particular, amorphous structures are fixed in rapidly quenched foils that belong to the concentration range from 17,5 to 40% Al in $La_{100-x}Al_x$ alloys with a "deep" eutectic concentration of 23%Al. This interval includes the composition of the intermediate compound La_3Al, as well as a very extended two-phase (La_3Al + LaAl) region of the state diagram of La-Al system. It is noteworthy that both of these phases belong to incongruent compounds, which, according to the data [12], increases the probability of noncrystalline solidification under QLS conditions. In-depth model studies of the kinetics of nonequilibrium crystallization of alloys of the class under consideration, similar to those performed previously for pure metals [17], are requiredto quantitatively estimate the effectiveness of the considered factor in the processes of formation of the structure of rapidly quenched alloys. Mathematical modeling using response surface methodology (RSM) of processing technologies of differential polymer materials is described in papers [18-20].

4. Conclusions

1. For alloys based on light rare-earth elements (La, Ce, Pr) with normal metals (Al, Cu, Ag), the critical values of the thickness (l_c=35-65 μm) and cooling rate (υ_c=1,8·10^5-1,1·10^6 K/s) of the melt layers experiencing non-crystalline solidification during quenching from the liquid state were determined.

2. It is shown that among the known metallic glasses studied alloys belong to the group of materials with an average level of glass-forming ability, which are obtained in the form of amorphous ribbons, foils or flakes with a thickness of 25-70 μm by various methods of rapid quenching.

3. X-ray diffraction patterns, as well as fine structure parameters (L, d_0) of rapidly quenched amorphous E-M alloys, correlate with the corresponding X-ray characteristics of metallic glasses of

other classes; that indicates the analogy of the atomic structure of amorphous phases fixed by quenching of metallic melts.

References

[1] Maslov V V, Paderno D Yu 1987 Obtaining of amorphous metal alloys *Amorphous metal alloys* pp 52-86.

[2] Filonov M R, Anikin Yu A and Levin Yu B 2006 *Theoretical foundations for the production of amorphous and nanocrystalline alloys by the method of superfast quenching* (Moscow: MISIS).

[3] Lysenko O B, Zagorulko I V and Kalinina T V 2020 Conditions for the fabrication of metallic glasses and truly amorphous materials *Progress in Physics of Metals* **21** pp 103-138.

[4] Tkatch V I, Limanovskii A I, Denisenko S N and Rassolov S G 2002 The effect of the melt-spinning processing parameters on the rate of cooling *Materials Science and Engineering* A323 pp 91-96.

[5] Lysenko A B, Borisova G V and Kravets O L 2004 Calculation of the cooling rate during quenching alloys from a liquid state *Physics and technology of high pressures* **14, 1** pp 44-53.

[6] Lysenko A B, Kosinskaya O L, Gubarev S V and Solovkov D V 2014 Dynamics of cooling during casting easily vitrified melts into a metal mold *Mathematical modeling* **30, 1** pp 58-62.

[7] Mardykin I P, Kashin V I and Sbitnev P P 1973 Thermal properties of lanthanum in solid and liquid states *Izv. Academy of Sciences of the USSR. Metals* **6** pp 77-80.

[8] Mardykin I P, Wertman A A 1972 Thermal properties of liquid cerium *Izv. Academy of Sciences of the USSR. Metals* **1** pp. 95-98.

[9] Mardykin I P, Kashin V I and Wertman A A 1973 Thermal properties of praseodymium in solid and liquid states *Izv. Academy of Sciences of the USSR. Metals* **4** pp 77-80.

[10] Miracle D B, Sanders W S and Senkov O N 2003 The influence of efficient atomic packing on the constitution of metallic glasses *Philosophical Magazine* **83, 20** pp 2409-2428.

[11] Chen H S 1980 Glassy metals *Reports on Progress in Physics* **43** pp 353-432.

[12] Slipchenko L S 1974 Formation of metastable states in alloys of iron, nickel, titanium and zirconium during rapid cooling of the melt: *dissertation abstract, Ph.D. in phys.-math. sciences: specialty 04.01.07 "Physics of the Solid State"* (Dnepropetrovsk).

[13] Lysenko A B 2009 Kinetics of the formation of metastable crystalline and amorphous phases during quenching from a melt and laser melting of the surface: *cand. for an apprenticeship doctoral degrees in physics and mathematics sciences: spec. 04.01.07 "Physics of the Solid State"* (Dnepropetrovsk).

[14] Skryshevsky A F 1980 *Structural analysis of liquids and amorphous alloys* (Moscow: Higher School).

[15] Gorelik S S, Skakov Yu A and Rastorguev L N 2002 *X-ray and electron-optical analysis* (Moscow: MISIS).

[16] Lysenko A B, Kravets O L and Lysenko A A 2009 Kinetic criterion of the propensity of metal melts to amorphization *Metallophysics and the latest technologies* **31, 10** pp 1311-1320.

[17] Lysenko A B, Borisova G V, Kravets O L and Lysenko A A 2008 Solidification of metals under melt quenching conditions *Physics of Metals and Metallography* **106, 5** pp 435-443.

[18] Dašić P 2019 *Response surface methodology*: *Selected scientific-professional papers* (in Serbian). SaTCIP Publisher Ltd., Vrnjačka Banja.

[19] Burya A I, Yeriomina Ye A, Volokh V I & Dašić P 2020 Study of the effect of transducer thickness and direction on the coercive force magnitude. *Lecture Notes in Networks and Systems (LNNS)*, 76: 229–237. doi: 10.1007/978-3-030-18072-0_26.

[20] Kalinichenko SV, Yeriomina Ye A, Burya AI & Dašić P 2020 Optimization of polychlorotrifluoroethylene processing technology by the response surface methodology. *Lecture Notes in Networks and Systems (LNNS)*, 128: 322–330. doi: 10.1007/978-3-030-46817-0_37.